

THEORETICAL ANALYSIS OF THE PISTON RING-PACK FOR PREDICTING FRICTION AND POWER LOSS IN AN INTERNAL COMBUSTION ENGINE


TEORIJSKA ANALIZA SKLOPA KLIPNOG PRSTENA RADI PROCENE GUBITAKA SNAGE USLED TRENJA U MOTORU SA UNUTRAŠNJIM SAGOREVANJEM


Originalni naučni rad / Original scientific paper
Rad primljen / Paper received: 19.07.2022

Adresa autora / Author's address:

¹⁾ Laboratoire des Systèmes Complexe (LSC), Ecole Supérieure en Génie Electrique et Energétique ESGEE Oran, Chemin Vicinal N9, Oran 31000, Algérie B. Menacer  0000-0002-7922-1847,

*email: menacer_brahim@esgee-oran.dz

²⁾ Department of Mechanics and Advanced Materials, Campus Monterrey, School of Engineering and Sciences, Tecnológico de Monterrey, Av. Eugenio Garza Sada 2501 Sur, Tecnológico, Monterrey 64849, Nuevo León, Mexico S. Narayan  0000-0001-6546-9086

³⁾ Department of Mechanical Engineering, Universidad de La Frontera, Temuco 4780000, Chile, V. Tuninetti  0000-0002-2808-0415

Keywords

- tribology
- finite difference method
- simulation algorithm
- dynamic piston ring
- lubrication
- GT-Suite®

Abstract

The piston ring is considered an essential element in the operation of the internal combustion engine to improve its efficiency and reduce its emissions. It is resistant to high temperature and high-pressure gases in the combustion chamber. A one-dimensional analysis method of lubrication between piston rings and cylinder liner in mixed lubrication conditions is developed in this article by using the GT-Suite simulation software. We applied the finite difference numerical method to solve the Reynolds equation to obtain the variation during an engine cycle of the following parameters; film thickness, frictional force, and power loss. The solution results presented can be used to improve the design of the piston ring pack in internal combustion engines and is available for industry usage.

INTRODUCTION

In internal combustion engines, the friction losses from the piston-ring-liner assembly vary between 50 and 75 % /1/ of the total friction losses produced during the operation of the engine. Given its importance in the engine's fuel consumption, we have developed a model that can predict the friction and power losses in the piston ring.

In the internal combustion engine, the piston rings perform several important tasks:

- eliminate clearance between piston and cylinder liner to conserve the combustion chamber pressure burnt gas and minimize blow-by;
- provide good cylinder surface lubrication to withstand high gas loads and forces at high speeds while maintaining acceptable lubricating oil consumption;
- keeping the piston temperature relatively low thanks to the heat transfer at the cylinder wall and also the coolant /2/.

From a technological point of view, there are two types of piston rings: the compression ring and the oil ring. Inter-

Ključne reči

- tribologija
- metoda konačnih razlika
- algoritam simulacije
- dinamički klipni prsten
- podmazivanje
- GT-Suite®

Izvod

Klipni prsten smatra se bitnim elementom u radu motora sa unutrašnjim sagorevanjem kako bi se poboljšala njegova efikasnost i smanjile emisije. Ovaj element je otporan na visoke temperature i visoke pritiske gasova u komori za sagorevanje. Metoda jednodimenzionalne analize podmazivanja između klipnih prstenova i košuljice cilindra u mešovitim uslovima podmazivanja, opisana u ovom članku, je razvijena korišćenjem simulacijskog softvera GT-Suite®. Primenili smo numeričku metodu konačnih razlika za rešavanje Reynoldsove jednačine kako bismo dobili varijaciju sledećih parametara u radnom ciklusu motora; debljina filma, sila trenja i gubitak snage. Rezultati predstavljeni u radu mogu se koristiti za poboljšanje dizajna sklopa klipnih prstenova u motorima s unutrašnjim sagorevanjem i dostupni su za industrijsku upotrebu.

nal combustion engines normally use three rings, two compression rings and an oil ring. For about fifty years, several researchers have tried to develop numerical models to describe the processes that occur in the ring-piston-liner assembly.

Takiguchi /3/ made an experimental study using a special piston that contains oil holes so that the amount of oil supplied to each ring is sufficient and ensures the formation of film thickness throughout the stroke and was able to see the development of frictional forces and the thickness of the oil film in the internal combustion engine. It has been found that at speed of 200 rpm, the frictional force is a non-hydrodynamic lubrication at the bottom dead centre (BDC), and for a speed of 4000 rpm, the peaks of friction forces at BDC disappear and are replaced by hydrodynamic lubrication throughout the engine's operating cycle.

Zhou et al. /4/ used stochastic theory to investigate the impact of ring surface roughness on lubrication and friction.

It was found that for a rough surface ($d = 0.6 \mu\text{m}$), the frictional power loss increases from about 8.3 to 9.4 %.

Sreenath et al. /5/ studied the influence of different engine loads on oil film thickness by resolving Reynold's equation and taking into account the effect of the squeeze film at top dead centre (TDC) and BDC, they compared their results with results from other researchers.

Abu-Nada et al. /6/ used a trigonometric function to approximate the shape of the oil film thickness where the oil film thickness takes minimum values at stroke ends (BDC and TDC) and higher values between both.

In this study, a numerical simulation program using the GT-Suite[®] software is elaborated to establish the piston ring-cylinder liner frictional model. We used mathematical models based on the one-dimensional Reynolds equation by assuming mixed boundary conditions to determine the hydrodynamic parameters such as friction and power loss for top compression ring, middle ring, and oil ring sliding against an engine cylinder liner.

THEORETICAL MODEL

The mathematical model used in this article is based on implicit assumptions to solve the one-dimensional Reynolds equation and find the pressure distribution in the oil film between the piston ring and the cylinder liner. The majority of research that studies the tribology of the ring-piston-liner assembly makes the following assumptions /7/:

- oil is assumed to be Newtonian and incompressible;
- oil viscosity does not vary along the ring face, although it may vary with temperature at different positions along the liner;
- there are no circumferential variations in oil film thickness (circumferential symmetry), but oil film thickness changes in-ring motion direction encourages the use of one-dimensional Reynolds equation;
- oil flow is laminar;
- there is no slippage at the boundaries;
- there is sufficient oil available for applying hydrodynamic equations /8/;
- oil film disruption may be accounted for by calculating the pressure distribution for a continuous oil film and then setting all negative pressures to zero, /9/.

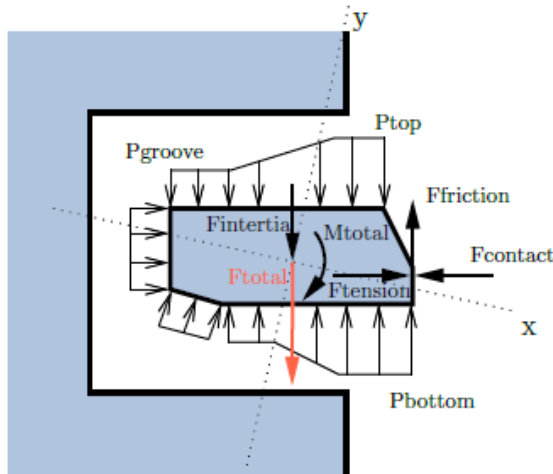


Figure 1. Description of forces influencing on piston ring, /11/.

During an operation cycle of a diesel engine, the piston ring motion is influenced by several types of forces and moments including (see Fig. 1): the gas pressure loads due to pressure difference; inertia loads due to piston acceleration and deceleration; friction loads due to ring contact with the cylinder liner; hydrodynamic forces and oil damping forces; forces due to asperities contacts; the tangential forces due to the pretension of the ring; contact forces between the piston ring and the piston, /10/.

Hydrodynamic lubrication model

One can use the Reynolds equation if there is a hydrodynamic lubrication model. This equation relates pressure and film shape as a function of oil viscosity and relative velocity. The oil film thickness is much smaller than the piston ring radius, so the simplified Reynolds equation is used, /12/:

$$\frac{\partial}{\partial x} \left(\phi_x \frac{h^3}{12\eta} \frac{\partial \bar{p}}{\partial x} \right) = \frac{U}{2} \frac{\partial \bar{h}_T}{\partial x} + \sigma \frac{U}{2} \frac{\partial \phi_s}{\partial x} + \frac{\partial \bar{h}_T}{\partial t}, \quad (1)$$

where: ϕ_x is the flow factor (a correction factor in the pressure-flow term to incorporate the effects of surface roughness); η is dynamic viscosity; \bar{p} is mean hydrodynamic pressure; U is relative sliding surface velocity; \bar{h}_T is averaged film thickness; and ϕ_s is shear factor (a correction factor applied to the additional flux term to compensate for the combined effect of sliding and roughness), /11/.

Using the boundary values of the flow factor /13/, the average Reynolds equation can therefore be written as:

$$\frac{\partial}{\partial x} \left(\frac{\rho h^3}{12\eta} \frac{\partial \bar{p}}{\partial x} \right) = \frac{U}{2} \frac{\partial \rho \bar{h}_T}{\partial x} + \frac{\partial \rho \bar{h}_T}{\partial t}, \quad (2)$$

where: ρ is the oil density.

Forces and moments meet in linear and angular momentum equations as follows, /14/:

$$F_x = m\ddot{x} = F_{g,x} + F_{h,x} + F_{a,x} + F_{k,x} + F_{fh,x} + F_{fa,x}, \quad (3)$$

$$F_y = m\ddot{y} = F_{g,y} + F_{h,y} + F_{a,y} + F_{k,y} + F_{fh,y} + F_{fa,y}, \quad (4)$$

$$M = I\ddot{\theta} = M_g + M_h + M_a + M_k + M_{fh} + M_{fa}, \quad (5)$$

where: \ddot{x} and \ddot{y} are the accelerations in directions x and y ; m is mass; I is the inertia moment; and $\ddot{\theta}$ is angular acceleration. In each time step, Newton's and Euler's equations are used to solve the forces and moments exerting on the piston surface, /17/.

The hydrodynamic force F_h , the mean hydrodynamic shear stress $\bar{\tau}$, and viscous friction F_{fh} exerting on area dA for each node i are given by the following equations:

$$F_h = \bar{p}dA, \quad (6)$$

$$\bar{\tau} = -\frac{\eta U}{h} (\sigma_f + \sigma_{fs}) + \sigma_f p \frac{h}{2} \frac{\partial \bar{p}}{\partial x}, \quad (7)$$

$$F_{fh} = \bar{\tau}dA. \quad (8)$$

Figure 2 presents the backward time and central space finite difference method for approximating the hydrodynamic pressure, /15, 16/:

$$\frac{1}{12\Delta x} \left(\frac{1}{2} \left(\left[\frac{\phi_x}{\mu} \right]_{i+1}^t + \left[\frac{\phi_x}{\mu} \right]_i^t \right) \left(\frac{h_{i+1} + h_i}{2} \right)^3 \left[\frac{P_{i+1}^t - P_i^t}{\Delta x} \right] - \left(\frac{1}{2} \left(\left[\frac{\phi_x}{\mu} \right]_i^t + \left[\frac{\phi_x}{\mu} \right]_{i-1}^t \right) \left(\frac{h_i + h_{i-1}}{2} \right)^3 \left[\frac{P_i^t - P_{i-1}^t}{\Delta x} \right] \right) =$$

$$= \frac{U}{2} \left(\frac{h_{T,i+1} - h_{T,i-1}}{2\Delta x} + \sigma_c \frac{\phi_{s,i+1} - \phi_{s,i-1}}{2\Delta x} \right) + \frac{h_{T,i}^t - h_{T,i-1}^{t-dt}}{\Delta t} \quad (9)$$

The general elimination method is used in this article to solve the above linear equation.

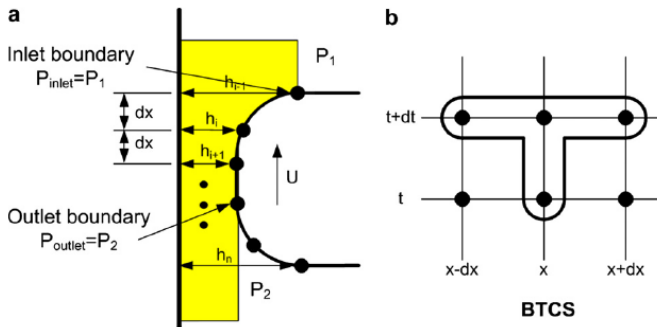


Figure 2. (a) calculation nodes on the piston ring surface and oil film thickness; (b) BTCS finite difference scheme for 1D Reynolds' equation solution, /17/.

Pure boundary lubrication model

If the oil supply has become insufficient, so then pure boundary lubrication (contact asperity) is used. It is described by Greenwood and Tripp's law /18/:

$$p_a = \frac{16\sqrt{2}\pi}{15} (\sigma_s \beta \eta_a)^2 E^* \sqrt{\frac{\sigma_s}{\beta}} F_{5/2}(h/\sigma_s), \quad (10)$$

$$F_a = p_a dA, \quad (11)$$

$$F_{fa} = C_f F_a, \quad (12)$$

where: \$\sigma_s\$ is the composite summit height standard deviation; \$\beta\$ is the radius asperity summit; \$\eta_a\$ is the surface density of asperity peaks; \$F_{5/2}(h/\sigma_s)\$ for Gaussian distribution surface and details of asperity contact are shown in /19/ and /20/; \$C_f\$ is the dry friction coefficient; and \$E^*\$ is the reduced elastic modulus:

$$\frac{2}{E^*} = \frac{1-\mu_1^2}{E_1} + \frac{1-\mu_2^2}{E_2}, \quad (13)$$

where: \$E_1\$ and \$E_2\$ are the elastic modules; \$\mu_1\$ and \$\mu_2\$ are Poisson's ratios of surfaces 1 and 2, respectively.

Mixed lubrication model

Mixed lubrication is considered between the pure hydrodynamic and pure boundary lubrication. The normal load \$F_M\$ and its friction \$F_{fM}\$ are carried by the hydrodynamic and boundary force components, /21/:

$$F_M = F_h + F_a, \quad (14)$$

$$F_{fM} = F_{fh} + F_{fa}. \quad (15)$$

The gas force \$F_g\$ which is exerting on area \$dA\$ of node \$i\$ is obtained from, /22/:

$$F_g = p_g dA. \quad (16)$$

The piston ring must be compressed to match the inside diameter of the liner. So the pretension force can be represented by the surface force /23, 24/:

$$F_k = p_k dA, \quad (17)$$

$$p_k = \frac{1}{2} \frac{Eb^3m}{l^2d(d-b)}, \quad (18)$$

where: \$E\$ is Young's modulus; \$b\$ is radial wall thickness; \$m\$ is total free gap; and \$d\$ is the nominal diameter.

SOLUTION METHOD

In this work, a numerical analysis is carried out on the study of hydrodynamic characteristics of the assembly piston-ring-cylinder liner in the single-cylinder diesel engine with direct injection using GT-Suite® software (the model is shown in Fig. 3). Our numerical model contains two main models; one is the piston-ring-cylinder friction model, and the other is the diesel engine working process model, and the latter provides the boundary conditions for the frictional model. There are three kinds of piston rings in the diesel engine; the first two rings are the compression rings, and the third segment is the oil control ring. Table 1 presents specific parameters of the three rings.

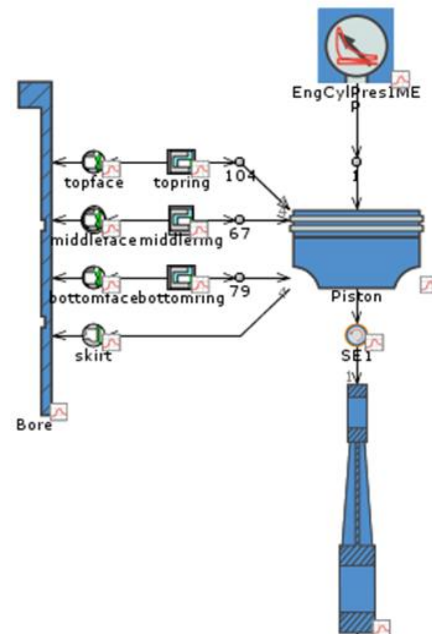


Figure 3. Piston-ring-cylinder liner friction model using GT-Suite® software /25/.

Table 1 shows main input data of the ring pack, the main engine parameters, and oil lubrication parameters.

Table1. Piston ring-cylinder liner structural parameters and performance indicators, /26/.

Main engine, ring pack and oil lubrication parameters	
cycle	Diesel 4 stroke
cylinder bore	120 mm
piston bore	119.5 mm
piston stroke	300 mm
mass of connecting rod	1900 g
length of connecting rod	
engine speed	2000 rpm
ring width:	
top ring, middle ring, oil ring	3.9; 3.9; 4.1 mm
ring mass:	
top ring, middle ring, oil ring	12.5; 9.0; 7.0 g
installed ring tension:	
top ring, middle ring, oil ring	50, 34, 44 N
ring gap clearance:	
top ring, middle ring, oil ring	0.22; 0.39; 0.49 mm
oil property object	SAE30
ring-cylinder friction coefficient	0.11
oil density	\$\rho = 900 \text{ kg/m}^3\$

RESULTS AND DISCUSSION

Figure 5 shows the change in oil film thickness of the top, middle and bottom ring at an engine speed of 2000 rpm and partial load. It can be seen that oil film thickness has higher values for the top ring and lower values for the middle ring. It can be viewed that the minimum film thickness for all the piston rings takes minimal values in the expansion period due to the increase of cylinder gas pressure in the combustion chamber. For the entire engine operating cycle, there is no break in the oil film at the TDC and BDC points.

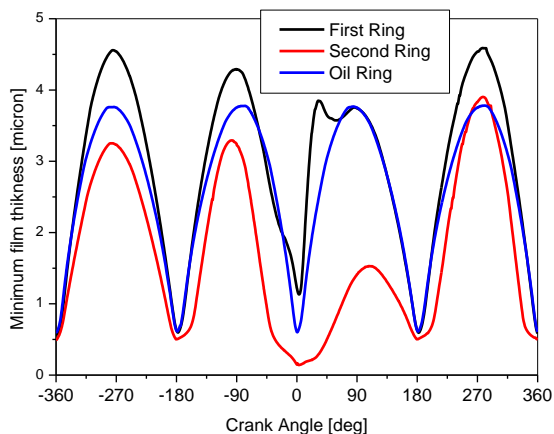


Figure 5. Cyclic variation of oil film thickness between piston rings and cylinder liner.

Figure 6 shows the variation in oil film pressure between piston ring and cylinder liner as a function of crankshaft angle for the three rings at 2000 rpm and partial load. The ring clearances and liner deformations have a great impact on oil film pressure values. In the combustion and expansion period, it can be shown that the top ring shows the highest value of maximal oil pressure, and the bottom ring shows the lowest maximal oil pressure.

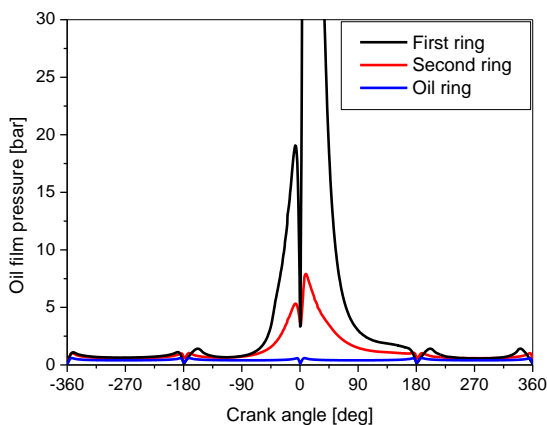


Figure 6. Cyclic variation of oil film pressure between piston rings and cylinder liner.

Figure 7 demonstrates the variation of the frictional force (incorporating hydrodynamic and boundary lubrication components) of the three piston rings with respect to the engine crankshaft angle at partial load and an engine speed of 2000 rpm. Negative values are due to the direction of piston velocity being changed by reciprocating motion. It is found that the highest values of friction force occur during the expansion stroke (from 0° to 180°) due to lack of lubricant

together with high combustion pressure forces, the top ring exhibits a peak of 39 N just after firing at TDC.

The comparison between the three piston rings showed that the top ring has the highest values of friction force in the expansion stroke (just after TDC firing), while the bottom ring shows the highest values of friction force at mid-stroke of the admission, compression, and exhaust strokes due to the enhancement of hydrodynamic friction. Finally, the middle ring showed the lowest values of friction force during the four strokes of the operating cycle.

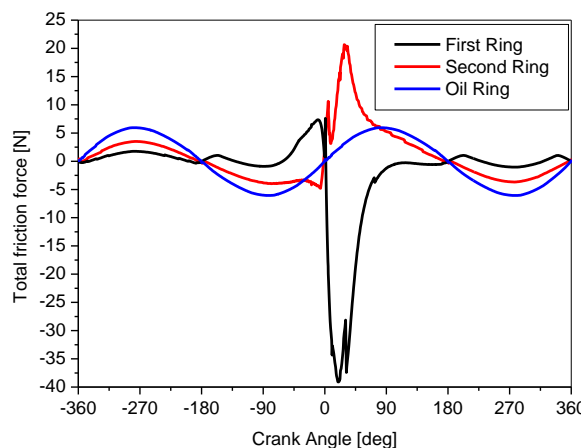


Figure 7. Cyclic variation of the total friction force between piston rings and cylinder liner.

Variation of the total power losses with crankshaft angle is visualized in Fig. 8 for different piston rings at partial load and engine speed of 2000 rpm. From this figure, it can be noticed that power losses reach their maximal values at mid-stroke and zero values at TDC and BDC, because the reciprocating speed of the piston reaches its maximal value and both oil film thickness and hydrodynamic shear increase at mid-stroke. The top piston ring has the maximum value of hydrodynamic friction power losses (about 0.138 kW) in the expansion stroke due to the increase in friction, while the bottom piston ring shows higher values of power losses which can reach up to 0.038 kW in the intake, compression and exhaust periods, due to the reduction in hydrodynamic friction. Also, concerning the power losses of the top and middle piston rings, the highest friction force values occurred during the expansion stroke.

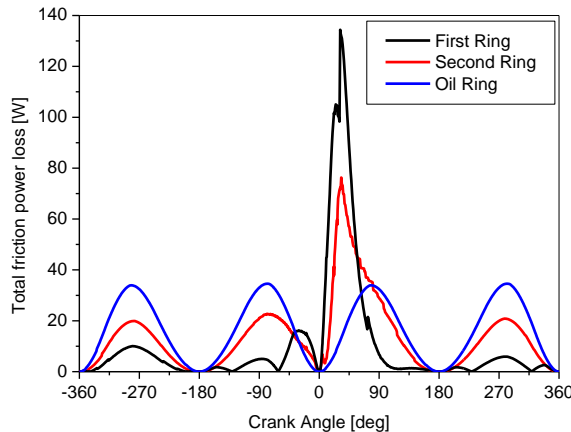


Figure 8. Cyclic variation of total friction force between piston rings and cylinder liner.

Variation of the twist angle for each ring is shown in Fig. 9. Maximal values of the twist angle appear in phases of piston motion corresponding to high values of gas pressure in the combustion chamber.

The variation of twist angle of the bottom ring is different from that in the top and middle rings. The twist angles of the top and middle rings change their sign, while the bottom ring has mainly the same sign of twist angle, because the gas forces practically do not influence bottom ring motion.

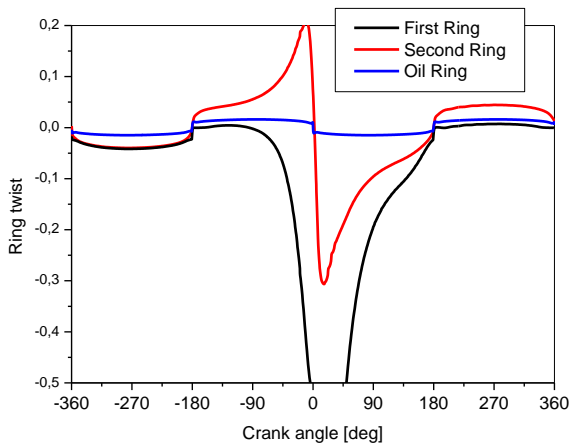


Figure 9 . Cyclic variation of ring twist between piston rings and cylinder liner.

Figure 10 demonstrates the variation of oil effective shear stress rate of the three piston rings with respect to engine crankshaft angle at partial load and an engine speed of 2000 rpm. For all rings, the maximum values of shear stress are at mid-stroke when the engine speed reaches its maximum value and zero at the TDC and BDC, respectively. In the intake, compression and exhaust periods, the bottom ring shows the highest values of shear stress, and the middle ring has the lowest values. In the expansion stroke, a peak of $1.3 \times 10^6 \text{ s}^{-1}$ is shown for the top ring.

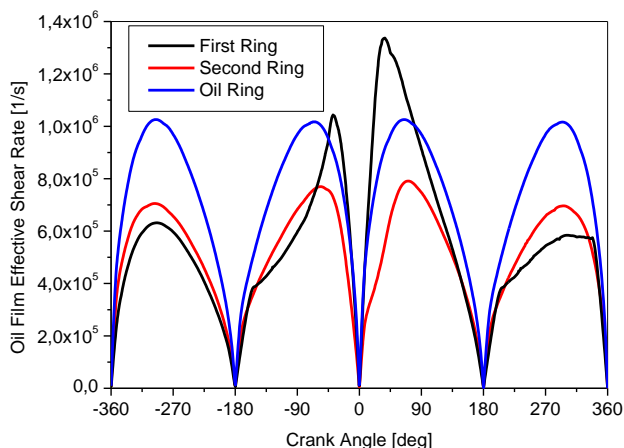


Figure 10. Cyclic variation of the oil effective shear stress rate between the piston rings and cylinder liner.

CONCLUSION

In the presented paper, we developed a one-dimensional mathematical model in order to obtain the main hydrodynamic performances between the three piston rings (top, middle, and oil control rings) and cylinder liner, the numer-

ical model is implemented using the GT-Suite[®] simulation software and the use of some assumptions. From the mathematical model developed in this study, several pieces of information can be concluded which are more complicated and expensive to obtain using experimental methods. The main phenomena can be noticed:

- the higher values of the minimum film thickness are given by the top ring;
- the top ring experienced higher values of maximum oil film pressure, the total friction force, and ring twist;
- for the expansion stroke, more friction power loss is viewed for the top ring;
- the bottom ring showed higher values of oil film effective shear rate for the intake, compression, and exhaust periods, but in the expansion period, the top ring presented the higher values of shear rate.

For future work of this type of study, we shall introduce new mathematical formulations on the pressure and flow conditions by involving the effects of surface roughness between the piston-ring-cylinder contact to make our simulation model more realistic, and for a better understanding of the hydrodynamic behaviour of friction loss in the piston ring assembly.

REFERENCES

1. Lechtape-Grüter, R., Kolbenringdynamik: dreidimensionale Finite-Elemente-Bewegungssimulation unter Berücksichtigung hydrodynamischer und gasdynamischer Wechselwirkungen, Dissertation, Lehrstuhl für Maschinenelemente und Tribologie, TU Kassel, 1995. ISBN 3-88122-815-2
2. Menacer, B., Bouchetara, M. (2020), *The compression ring profile influence on hydrodynamic performance of the lubricant in diesel engine*, Adv. Mech. Eng. 12(6): 1-13. doi: 10.1177/1687814020930845
3. Harigaya, Y., Suzuki, M., Takiguchi, M. (2003), *Analysis of oil film thickness on a piston ring of diesel engine: effect of oil film temperature*, J Eng. Gas Turbines Power, 125(2): 596-603. doi: 10.1115/1.1501078
4. Zhou, Q.-B., Zhu, T.-Z., Wang, R.-S. (1988), *A full lubrication model for rough surface piston rings*, Tribol. Int. 21(4): 211-214. doi: 10.1016/0301-679X(88)90019-9
5. Sreenath, A.V., Venkatesh, S. (1973), *Analysis and computation of the oil film thickness between the piston ring and cylinder liner of an internal combustion engine*. Int. J Mech. Sci. 15(8): 605-611. doi: 10.1016/0020-7403(73)90093-3
6. Abu-Nada, E., Al-Hinti, I., Al-Sarkhi, A., Akash, B. (2008), *Effect of piston friction on the performance of SI engine: A new thermodynamic approach*, J Eng. Gas Turbines Power, 130(2): 022802. doi: 10.1115/1.2795777
7. Ejakov, M.A., Schock, H.J., Brombolich, L.J. (1998), *Modeling of ring twist for an IC engine*, SAE Tech. Paper 982693. doi: 10.4271/982693
8. Tian, T. (2002), *Dynamic behaviours of piston rings and their practical impact. Part 1: Ring flutter and ring collapse and their effects on gas flow and oil transport*, Proc. Inst. Mech. Eng. Part J: J Eng. Tribol. 216(4): 209-228. doi: 10.1243/135065002760199961
9. Tian, T. (2002), *Dynamic behaviours of piston rings and their practical impact. Part 2: Oil transport, friction and wear of ring/liner interface and the effects of piston and ring dynamics*, Proc. Inst. Mech. Eng. Part J: J Eng Tribol. 216(4): 229-248. doi: 10.1243/135065002760199970

10. Thirouard, B., Tian, T. (2003), *Oil transport in the piston ring pack (Part I): Identification and characterization of the main oil transport routes and mechanisms*, SAE Tech. Paper 2003-01-1952. doi: 10.4271/2003-01-1952
11. Andersson, P., Tamminen, J., Sandström, C.-E. (2002), *Piston ring tribology: A literature survey*, Tech. Res. Centre of Finland. VTT Tiedotteita - Research Notes No. 2178 <https://publications.vtt.fi/pdf/tiedotteet/2002/T2178.pdf>
12. Herbst, H.M., Priebisch, H.H. (2000), *Simulation of piston ring dynamics and their effect on oil consumption*, SAE Tech. Paper 2000-01-0919. doi: 10.4271/2000-01-0919
13. Novotný, P., Pištěk, V., Drápal, L. (2011), *Modeling of piston ring pack dynamics*, MECCA J Mid. Europ. Constr. Des. Cars, 9(2): 8-13. doi: 10.2478/v10138-011-0008-y
14. Mittler, R., Mierbach, A., Richardson, D. (2009), *Understanding the fundamentals of piston ring axial motion and twist and the effects on blow-by*, In: Proc. ASME 2009 Int. Combustion Engine Dev. Spring Tech. Conf., Milwaukee, Wisconsin, USA, 2009, Paper No: ICES2009-76080: 721-735. doi: 10.1115/ICE S2009-76080
15. Shahmohamadi, H., Mohammadpour, M., Rahmani, R., et al. (2015), *On the boundary conditions in multi-phase flow through the piston ring-cylinder liner conjunction*, Tribol. Int. 90: 164-174. doi: 10.1016/j.triboint.2015.04.025
16. Maassen, F.J., Dohmen, J., Pischinger, S., Schwaderlapp, M. (2005), *Engine friction reduction, Design measures for reduced fuel consumption*, MTZ Worldw. 66: 30-33. doi: 10.1007/BF03227776
17. Wannatong, K., Chanchaona, S., Sanitjai, S. (2008), *Simulation algorithm for piston ring dynamics*, Simul. Modell. Pract. Theory, 16(1): 127-146. doi: 10.1016/j.simpat.2007.11.004
18. Greenwood, J.A., Tripp, J.H. (1970), *The contact of two nominally flat rough surfaces*, In: Proc. Inst. Mech. Eng. 185(1): 625-633. doi: 10.1243/PIME_PROC_1970_185_069_02
19. Yun, J.E., Chung, Y., Chun, S.M., Lee, K.Y. (1995), *An application of simplified average Reynolds equation for mixed lubrication analysis of piston ring assembly in an internal combustion engine*, SAE Tech. Paper 952562. doi: 10.4271/952562
20. Arcoumanis, C., Ostovar, P., Mortler, R. (1997), *Mixed lubrication modelling of Newtonian and shear thinning liquids in a piston-ring configuration*, SAE Tech. Paper 972924. doi: 10.4271/972924
21. Jeng, Y.R. (1992), *Theoretical analysis of piston-ring lubrication Part I-Fully flooded lubrication*, Tribol. Trans. 35(4): 696-706. doi: 10.1080/10402009208982174
22. Lyubarskyy, P., Bartel, D. (2016), *2D CFD-model of the piston assembly in a diesel engine for the analysis of piston ring dynamics, mass transport and friction*, Tribol. Int. 104: 352-368. doi: 10.1016/j.triboint.2016.09.017
23. Furuhashi, S. (1959), *A dynamic theory of piston-ring lubrication: 1st Report, Calculation*, Bull. JSME, 2(7): 423-428. doi: 10.1299/jsme1958.2.423
24. Furuhashi, S. (1960), *A dynamic theory of piston-ring lubrication: 2nd Report, Experiment*, Bull. JSME, 3(10): 291-297. doi: 10.1299/jsme1958.3.291
25. Gamma Technologies, LLC[®]: *GT-POWER User's Manual version 7.4*, September 2016.
26. Shi, C.-F., Wang, P.-K., Liu, J.-M., et al. (2018), *Research of the frictional characteristics of piston ring-cylinder liner based on GT-Suite*, MATEC Web of Conferences, 179(2): 01020. doi: 10.1051/mateconf/201817901020

© 2024 The Author. Structural Integrity and Life, Published by DIVK (The Society for Structural Integrity and Life 'Prof. Dr Stojan Sedmak') (<http://divk.inovacionicentar.rs/ivk/home.html>). This is an open access article distributed under the terms and conditions of the [Creative Commons Attribution-NonCommercial-NoDerivatives 4.0 International License](https://creativecommons.org/licenses/by-nc-nd/4.0/)